



Analysis of the changing patterns of seasonal flooding along the U.S. East Coast

Tal Ezer¹

Received: 16 August 2019 / Accepted: 8 November 2019 / Published online: 26 November 2019
© Springer-Verlag GmbH Germany, part of Springer Nature 2019

Abstract

Sea level rise (SLR) is causing acceleration in the frequency and duration of minor tidal flooding (often called “sunny-day” or “nuisance” flooding) along the U.S. East Coast. Those floods have a seasonal pattern that often follows the monthly mean sea level anomaly which peaks in September–October for stations between New York and south Florida. However, there are large differences between coasts: for example, over 75% of the minor floods occur during the fall in Florida, but during the spring and winter in Boston. Various data and forcing, such as tide gauge records, surface temperatures, winds, long-term tidal cycles, and the Gulf Stream flow, were analyzed to examine potential drivers and mechanisms that can contribute to the seasonal pattern of floods. The seasonal water temperature cycle, with maximum temperatures in August, could not by itself explain the seasonal sea level pattern, but two mechanisms that significantly correlate with the seasonal sea level and flooding patterns are the annual and semi-annual tidal cycles (correlation of ~ 0.97) and changes in the Gulf Stream (GS) flow (correlation of -0.6 ; the GS shows a maximum decline in September–October during the period of peak flooding). The combination of the seasonal pattern of tropical storms and high coastal sea level can explain the high frequency of fall flooding along the Southeastern U.S. coasts, while winter storms have more influence on the northeastern coasts. In recent decades however, the seasonal pattern seemed to have shifted so that increased flooding is seen on the northeastern coasts during spring and summer, while in the Mid-Atlantic and southeastern coasts, a dramatic increase in flooding is seen almost exclusively during the fall. A long-term change in the mean zonal wind pattern along the coast can contribute to the recent shift in the seasonal flooding pattern. The study can help regional adaptation and resilience planning for flood-prone coastal cities and communities.

Keywords Coastal sea level · Flooding · U.S. East Coast · Climate change · Seasonal variations

1 Introduction

Local sea level rise (SLR) rates along the U.S. East Coast are generally larger than the global rate due to regional land subsidence, and the rates seem to accelerate in recent decades (Boon 2012; Ezer and Corlett 2012; Sallenger et al. 2012). With rising seas, the frequency and severity of coastal flooding is accelerating as well, from Boston to south Florida (Ezer and Atkinson 2014; Sweet and Park 2014;

Kruel 2016; Wdowinski et al. 2016). In particular, minor flooding (the so-called nuisance floods or sunny day floods; Sweet et al. 2014, 2018) increased dramatically in recent years since even weak storms or normal Spring Tides that had no impact in the past can now push water above the threshold flood level at many places; the definition and values of nuisance floods at different locations are further discussed in the next section. Numerous studies investigated the spatial variations in SLR and associated flooding along the coast, as well as the interannual and decadal variations of sea level and their relation to various factors, such as wind and pressure patterns (Piecuch et al. 2016; Woodworth et al. 2016; Valle-Levinson et al. 2017), thermal anomalies (Domingues et al. 2018; Ezer 2019b), the Atlantic Meridional Overturning Circulation, AMOC (Ezer 2015; Goddard et al. 2015; Caesar et al. 2018; Piecuch et al. 2019), and variations in the Gulf Stream (Ezer et al. 2013; Park and Sweet 2015; Ezer 2013, 2016, 2018).

Along the U.S. East Coast, one can find significant spatial variations in sea level variability and sea level rise rates which

This article is part of the Topical Collection on the *11th International Workshop on Modeling the Ocean (IWMO)*, Wuxi, China, 17–20 June 2019

Responsible Editor: Fanghua Xu

✉ Tal Ezer
tezer@odu.edu

¹ Center for Coastal Physical Oceanography, Old Dominion University, 4111 Monarch Way, Norfolk, VA 23508, USA

in turn will affect flood patterns. However, there is also a large coherency in sea level variability within each sub-region, for example, in the Gulf of Maine (GOM), in the Mid-Atlantic Bight (MAB), and in the South Atlantic Bight (SAB). For example, the SAB and the MAB often show different sea level variability due to regional wind forcing, different topographic features, and distance between the coast and the Gulf Stream (Woodworth et al. 2016; Ezer and Atkinson 2017; Valle-Levinson et al. 2017; Domingues et al. 2018; Ezer 2019b). On seasonal time scales, spatial variations of forcing and impact on coastal sea level can be significant due to latitudinal changes in atmospheric and oceanic conditions, tides, and coastline topography.

Unlike sea level variations on timescales of years and longer, less attention is given to intra-annual variations and the seasonal cycle of sea level and flooding. Sweet et al. (2014) for example, show clear seasonal pattern of nuisance flooding, with winter-time maximum in the Pacific coasts of the U.S. and along the U.S. northeast Atlantic coasts, while a fall-time maximum is found along the Mid-Atlantic coasts. Sweet et al. pointed out that different regions are affected by different forcing, though the nuisance flooding is closely related to the seasonal cycle of mean local sea level. Many factors have seasonal cycle that can affect flooding patterns, such as storm surges during the hurricane season (including tropical cyclones/storms) affecting the southeastern coast of the U.S. and wintertime nor'easter storms (extratropical cyclones) affecting the Mid-Atlantic coasts. The seasonal pattern of winds, temperatures and tides are also considered here, but other potential influences on sea level such as contributions from rivers and precipitation are beyond the scope of this study. The main goal in this study is to systematically evaluate the influence of various factors on the intra-annual variations of flooding (nuisance and more severe ones) and to examine the potential contribution of each factor. Long-term changes in the seasonal pattern of floods are also investigated for potential impact from climate change.

The study is organized as follows. First, the data sources and analysis are described in Section 2, then results are presented in Section 3, and finally, a summery and conclusions are offered in Section 4.

2 Data sources and analysis

Ten tide gauge stations are used, 2 in the Gulf of Maine, 3 in the Mid-Atlantic Bight, 4 in the South Atlantic Bight, and 1 in Key West, Florida (see Fig. 1 and Table 1). Hourly water levels were obtained from NOAA (<http://opendap.co-ops.nos.noaa.gov/dods/>). Water level data in those locations have almost continuous records for at least 1935–2018. For each station, annual flood hours were calculated by summing up the hours when water level reached the nuisance level defined

by NOAA (Sweet et al. 2014, 2018) and shown in Table 1. NOAA determines these levels based on the history of documented past minor coastal flooding at each location. However, when considering local rainfall or wind, impacts can become more severe and reach moderate or major flood levels, so nuisance flood level provides only a general measure that can be used to guide local communities at risk. Note that for easier comparisons between different locations, in some studies (e.g., Ezer and Atkinson 2014), minor, moderate, and major flood levels were defined at fixed levels of 0.3, 0.6, and 0.9 m, respectively, above mean higher high water (MHHW), rather than setting different flood levels for each station as NOAA does. Nevertheless, the main pattern of accelerated flooding does not significantly change when slightly different definitions of flood levels are used (e.g., Sweet and Park 2014 versus Ezer and Atkinson 2014).

Monthly means, standard deviations, and monthly maxima of water levels were calculated from the hourly data for each station. The standard deviation mostly represents the tidal range while the monthly maximum represents mostly storm surges. The daily Florida Current (FC) transport across the Florida Strait (Baringer and Larsen 2001; Meinen et al. 2010) was obtained from NOAA's Atlantic Oceanographic and Meteorological Laboratory (www.aoml.noaa.gov/phod/floridacurrent/). Monthly sea surface temperatures and zonal winds were obtained from NOAA/NCEP reanalysis (<https://www.esrl.noaa.gov/psd/data/gridded/data.ncep.reanalysis.html>). To extract annual and semi-annual tidal constituents, the U-TIDE Matlab code (Codiga 2011) was used; this code is based on the T-TIDE code developed and described by Pawlowicz et al. (2002).

3 Results

3.1 The spatial and temporal distribution of the seasonal nuisance flooding

To capture seasonal mean values, the following 4 seasons were defined: winter (December–February), spring (March–May), summer (June–August), and fall (September–November). Regardless of the total flood hours at each location (discussed later), it is instructive to look first at the distribution of flooding at the 10 locations, and the result clearly shows a latitudinal trend (Fig. 2). In the north (GOM), ~75% of the floods occurred during winter and spring (dark and light blue, respectively, in Fig. 2), but this share of the flooding is gradually decreasing as one moves south along the coast, to ~50% in Delaware, ~33% in Virginia, ~27% in South Carolina, and ~5–10% in Florida. On the other hand, the fall flooding (yellow in Fig. 2) is maximum in the south (75–92% of the flooding in Florida) and gradually decreasing as one moves north along the coast, to ~60% in Virginia, ~40% in

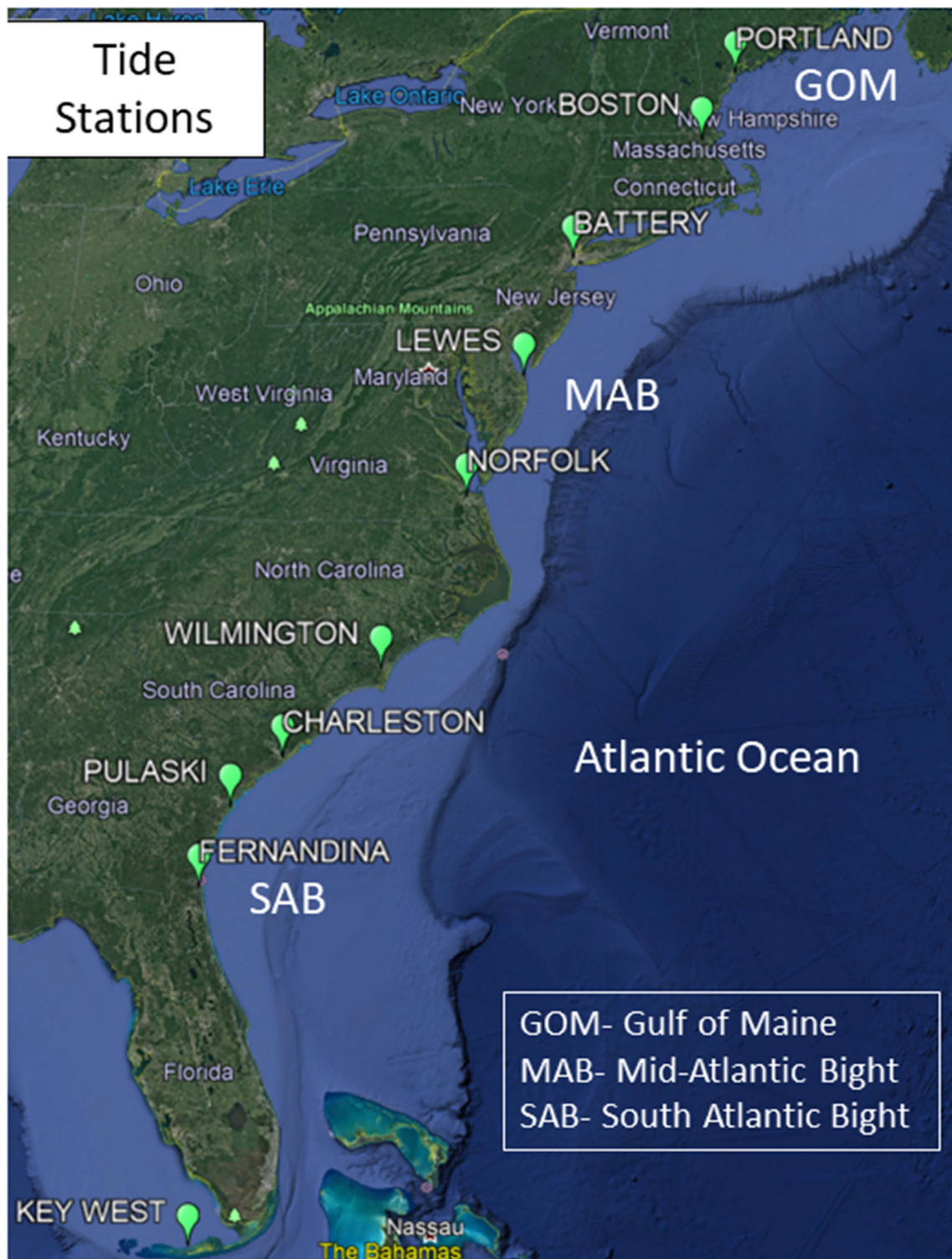


Fig. 1 A map of the U.S. East Coast and locations of the 10 tidal stations used in this study

New York, and only ~ 14% in Boston and Portland. Therefore, forcing mechanisms that are a function of latitude and have a seasonal cycle (e.g., temperatures and winds) are analyzed in this study to examine how they may influence this spatial pattern.

To prepare coastal communities to the impact of climate change (and sea level in particular), it is important to see if the seasonal pattern of flooding described above is a permanent characteristic or if it has changed over time. Figure 3 thus shows the relative change in the seasonal pattern of Fig. 2

Table 1 The tide gauge data used in this study, their location, starting record, mean sea level rise (SLR; from <https://tidesandcurrents.noaa.gov/>), and nuisance flood level (Sweet et al. 2014)

Station	Latitude (°N)	Longitude (°W)	Start (year)	SLR (mm/y)	Nuisance flood level (m above MHHW)
Portland, ME	43.66	70.25	1910	1.88	0.68
Boston, MA	42.35	71.05	1921	2.83	0.68
Battery, NY	40.70	74.01	1920	2.85	0.5
Lewes, DE	38.78	75.12	1920	3.48	0.41
Norfolk, VA	36.95	76.33	1927	4.66	0.53
Wilmington, NC	34.23	77.95	1935	2.39	0.25
Charleston, SC	32.78	79.93	1921	3.26	0.38
Ft. Pulaski, GA	32.03	80.90	1935	3.25	0.46
Fernandina, FL	30.67	81.47	1940	2.11	0.59
Key West, FL	24.56	81.81	1920	2.42	0.33

between the years before 1990 and after 1990. This year was chosen, since the 1990 seemed close to an inflection point when minor flooding started a significant upward trend (Ezer and Atkinson 2014; Sweet and Park 2014). The change after 1990 relative to previous times before 1990 shows distinct regional pattern. In the north (Portland and Boston), proportional summer flooding increased by 10–15% while winter flooding decreased by 10–15%. Note that while the total annual hours of flooding generally increased everywhere and at most seasons (see later), this percentage is a relative number to show only the shift between seasons. The largest changes are seen in Norfolk (MAB) and Wilmington (SAB) where relative fall flooding increased 12–22% while spring flooding decreased by more than 20% (Key West saw the 3rd largest increase in relative fall's flooding, ~8%).

It is clear from Fig. 3 that variations in the seasonal flooding significantly change from place to place and over time, so it is not likely that a single mechanism affects flooding patterns along the entire U.S. East Coast. Therefore, the flooding pattern at several individual locations is examined in Figs. 4, 5, 6, 7, and 8. Minor flooding in Boston (Portland, not shown, has similar pattern; see Figs. 2 and 3) occurred mostly in winter and spring (Fig. 4a, b). In fact, summer flooding was almost non-existence before ~2008 (Fig. 4c), and fall flooding was small with very little change since the 1940s (Fig. 4d). The trend may indicate a recent shift to relatively more spring and summer flooding and a smaller change during winter. A potential explanation is that the frequency of winter storms in this region is not changing much, while rising in sea surface temperatures and sea level during summer brought water levels to the threshold of nuisance water level only recently. Studies of extreme winter climate and extratropical cyclones over the Northeastern U.S. (Ning and Bradley 2015; Hall and Booth 2017) show strong influence from climate modes such as the North Atlantic Oscillation (NAO) and El Niño–Southern Oscillation (ENSO), which could explain the large interannual variations in winter flooding seen in Boston (Fig. 4a) and New York

(Fig. 5a). Flooding in New York (Fig. 5) has similar pattern to Boston during winter, spring, and summer, but a much larger increase in fall flooding is seen (Fig. 5d; up to 25 h of fall flooding in New York, compared to less than 5 h in Boston). In the MAB (at Norfolk, Fig. 6) and SAB (at Charleston, Fig. 7), the largest increase in nuisance flooding in recent years is mostly seen during the fall. Higher fall sea levels in these locations are affected by tropical storms and hurricanes through both, direct storm surges and indirect impacts of storms on weakening of the Gulf Stream (Ezer 2018, 2019a). In the southernmost point, at Key West (Fig. 8), flooding occurred almost exclusively during the fall, and before the 1990s, nuisance flooding was almost non-existing year-round.

3.2 Monthly mean sea level, sea surface temperature, and Gulf Stream transport

It has been suggested that the seasonal pattern of nuisance flooding is closely related to the monthly mean sea level (Sweet et al. 2014). Various factors, such as water temperatures and winds, have seasonal variations that can affect the mean sea level. Examples of the monthly mean, standard deviation, and maximum sea level are shown in Fig. 9. The standard deviation represents the tidal range, showing large tidal range (~2 m) in Boston and much smaller (~0.2 m) in Key West (note the different y-axis scales in Fig. 9). The maximum monthly sea level represents storm surges, with peak in winter-spring time (especially in Boston and Norfolk) and in September–October at all stations. However, while the maximum sea level in the fall occurred at the same time when monthly mean sea level is high, the maximum sea level in the winter and spring occurred when monthly mean sea level is relatively low, so the relation between mean and maximum sea level is not straight forward. Also, cause and effect cannot be inferred from this relation: on the one hand, higher mean sea level can cause larger storm surges and more

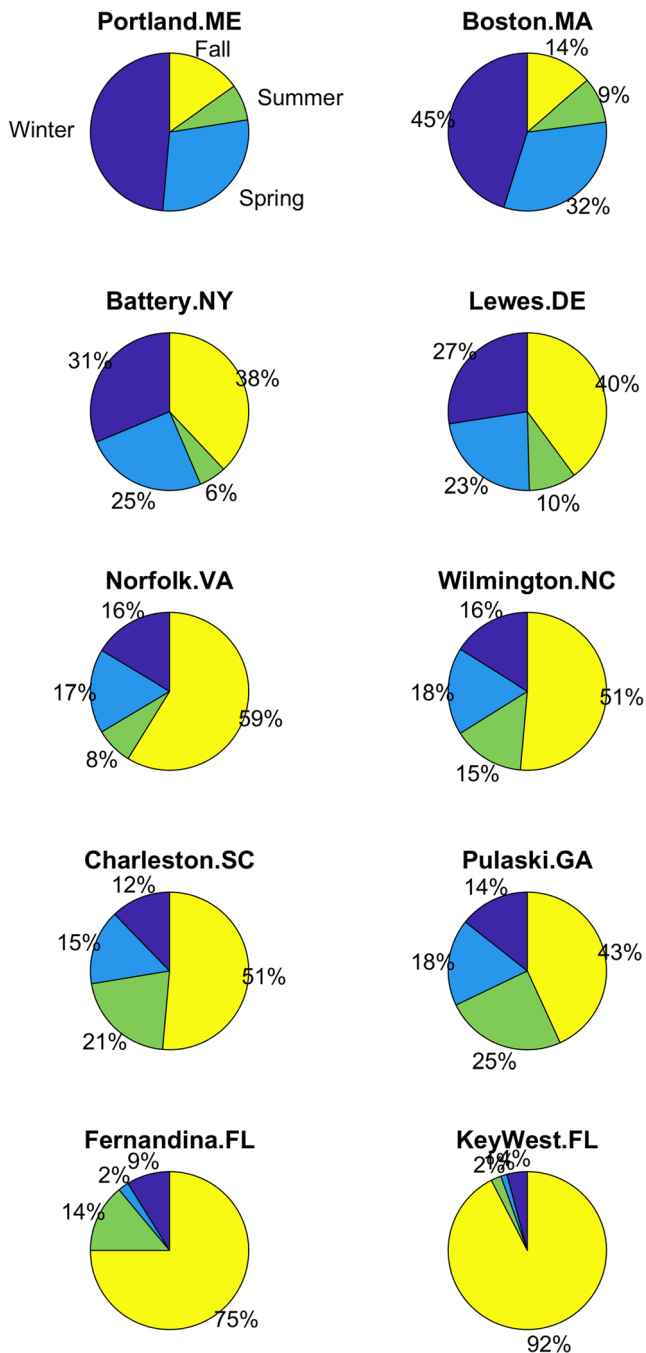


Fig. 2 The seasonal relative distribution of nuisance floods as a percentage of the total annual hours of floods for winter (December–February; dark blue), spring (March–May; light blue), summer (June–August; green), and fall (September–November; yellow)

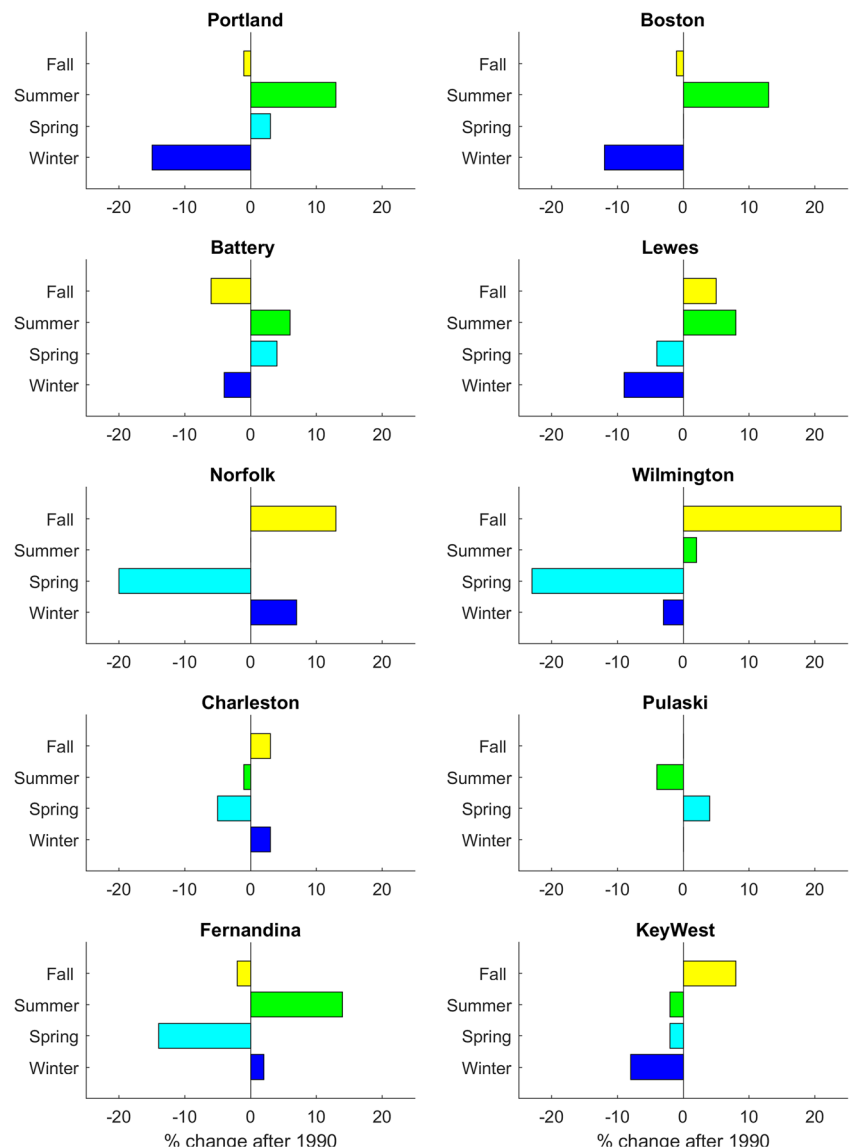
flooding, but on the other hand, more frequent storm surges during the fall can cause higher mean sea level then.

Mean sea level anomaly is quite similar at all locations between Norfolk and Key West (black heavy lines in Fig. 9c–f) and can reach a maximum anomaly of ~ 15 cm during September–October. In the northern coasts, seasonal changes of the monthly mean anomaly are much smaller and insignificant relative to the large tides (Fig. 9b). To examine the

hypothesis that the seasonal cycle of mean sea level is driven by thermal expansion due to the ocean’s seasonal temperature changes, the monthly mean sea surface temperature (SST) in the western North Atlantic near the coast is shown in Fig. 10a. The annual range of SST varies between a maximum of ~ 20 °C at 39° N (near the Lewes station) and a minimum of ~ 5 °C at 24° N (near the Key West station); in all locations, SST is maximum in August and minimum in February–March. Since the timing of the maximum SST and the variations of SST range with latitude in Fig. 10a are inconsistent with the variations in the mean sea level in Fig. 9, it is unlikely that mean coastal sea level is driven primarily by thermal expansion. Summer SST warming can contribute to higher sea level but cannot explain why the maximum sea level is found in September–October and not in August. Note that variations in sea surface height due to thermal expansion are more closely related to the heat content of the upper ocean rather than SST. However, in the shallow places where the tide gauges are located the water is quite well mixed, so the change in heat content can be estimated as $\Delta HC = \rho C_p H \Delta T$, where ρ is the average density, C_p is the specific heat constant, H is the depth, and ΔT is the change in temperature of the upper layer. Therefore, changes in SST, which are close to changes in the mean temperature in shallow areas, should be proportional to changes in the heat content and the thermal expansion effect.

Another potential driver of coastal sea level is the Gulf Stream (GS)—numerous recent studies show that weakening in the GS flow is associated with rising water levels along the U.S. East Coast (Ezer 2013, 2015, 2016, 2018; Park and Sweet 2015; Wdowinski et al. 2016); this is the result of the geostrophic balance where the sea level slope across the GS is proportional to the flow speed. Note that in the MAB, a shift offshore in the position of the GS can also cause an increase in the southward flowing Slope Current and an increase in coastal sea level (see Fig. 2 in Ezer et al. 2013). On time scales from days to decades, sea level variability often has higher anti-correlation with changes in the GS transport rather than with the strength of the current itself (see Fig. 10 in Ezer et al. 2013 and Fig. 9 in Ezer and Atkinson 2017). Figure 10b shows the monthly mean transport of the Florida Current (FC) at 27° N (Baringer and Larsen 2001; Meinen et al. 2010), calculated from the cable data for 1982–2018; the FC is the upstream, southern portion of the GS which flows along the Florida coast. The maximum transport is in July and minimum in November with seasonal variations of ~ 2–3 Sv (1 Sverdrup = $10^6 \text{ m}^3 \text{ s}^{-1}$). The large standard deviation (SD) indicates large variability in the daily data due to both, high-frequency and interannual variations (Meinen et al. 2010). Between March and July transport is generally increasing while from July to November transport is dropping. A comparison between the month to month change in transport and variations in sea level in Norfolk (Fig. 10c) shows a correlation of -0.6 (at 97% confidence level); similar high

Fig. 3 The relative percentage change in the seasonal flooding between the period before 1990 and after 1990. The colors for each season are the same as in Fig. 2. The total % of change at each station is zero



correlations are seen for other stations in the MAB and SAB. Note in particular that the largest drop in the Florida Current transport occurred in September–October, when monthly sea level is maximum in most stations, while a large increase in FC transport between January and February coincides with minimum sea level in most stations (Fig. 9). The results are consistent with the previously found anti-correlation between variations in GS strength and interannual and decadal variations in sea level anomaly (Ezer et al. 2013), but here, it is demonstrated that this relation applies also to monthly mean seasonal changes.

3.3 The contribution from the annual and semi-annual tidal cycles

Other potential forcing mechanisms that can contribute to seasonal variations in coastal sea level are long-term tidal cycles,

and in particular the solar annual constituent (S_a) with a period of 365.25 days and the semi-annual constituent (S_{sa}) with a period of 182.62 days; these cycles result from variations in the distance between the Earth and the Sun over the year and variations in the solar declination. These long tidal cycles can cause higher than normal water levels along the Southeastern U.S. coast during the fall and an increase in minor tidal flooding when the spring tide is combined with the high phase of the S_a and S_{sa} tides. The (unscientific) term “King Tide” is often used to describe this period of unusual tidal flooding; for example, in the flood-prone Hampton Roads region of Virginia, an annual citizen science event, “Catch the King Tide” (https://www.vims.edu/people/loftis_jd/Catch%20the%20King/index.php), is held when hundreds of volunteers monitor and map flooded streets and help improve inundation models (Loftis et al. 2018). This “King Tide” event in October–November 2017 is seen in Fig. 11b,

Fig. 4 The annual hours of nuisance floods for each season (as defined in Fig. 2) for Boston, MA

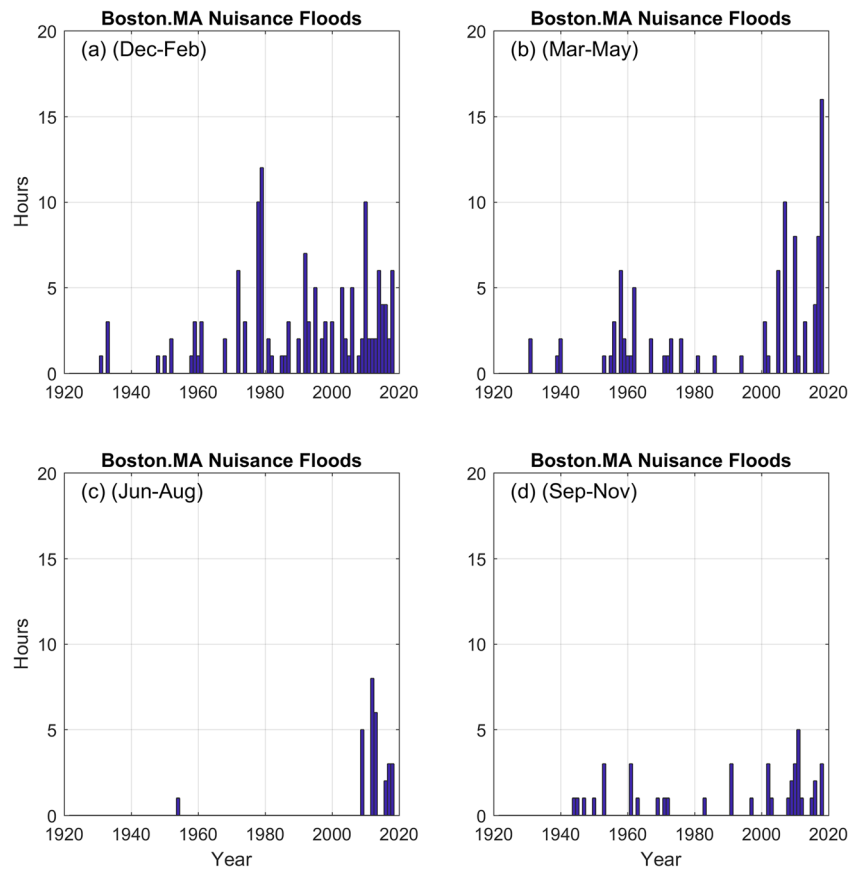


Fig. 5 Same as Fig. 4, but for Battery, NY

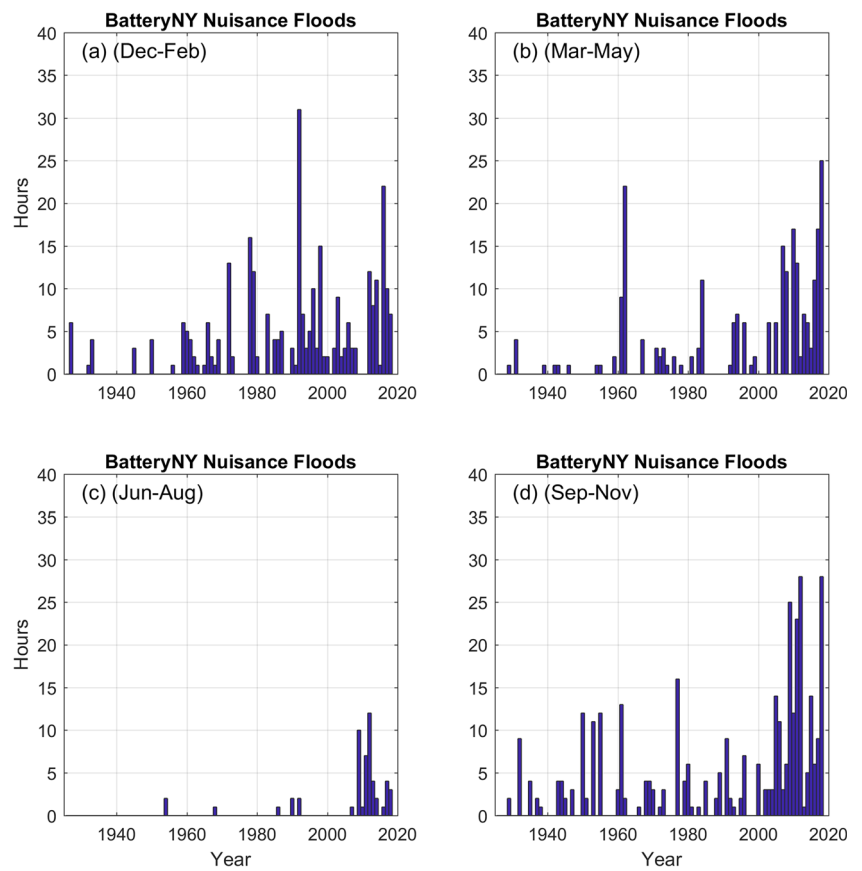


Fig. 6 Same as Fig. 4, but for Norfolk (Sewells Point), VA

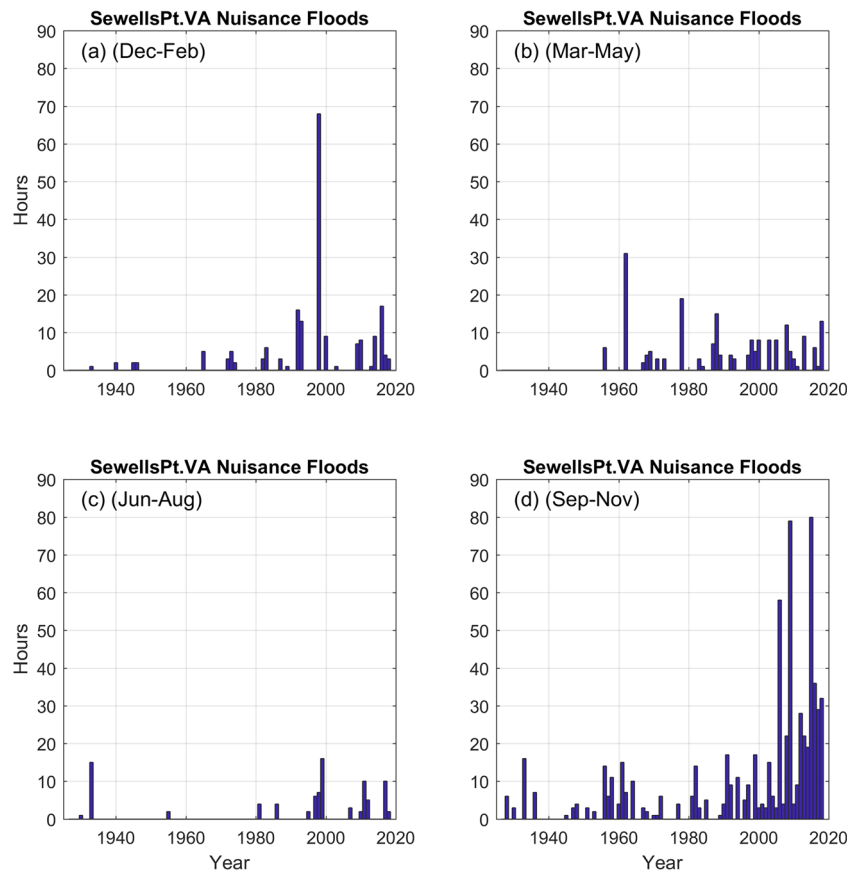


Fig. 7 Same as Fig. 4, but for Charleston, SC

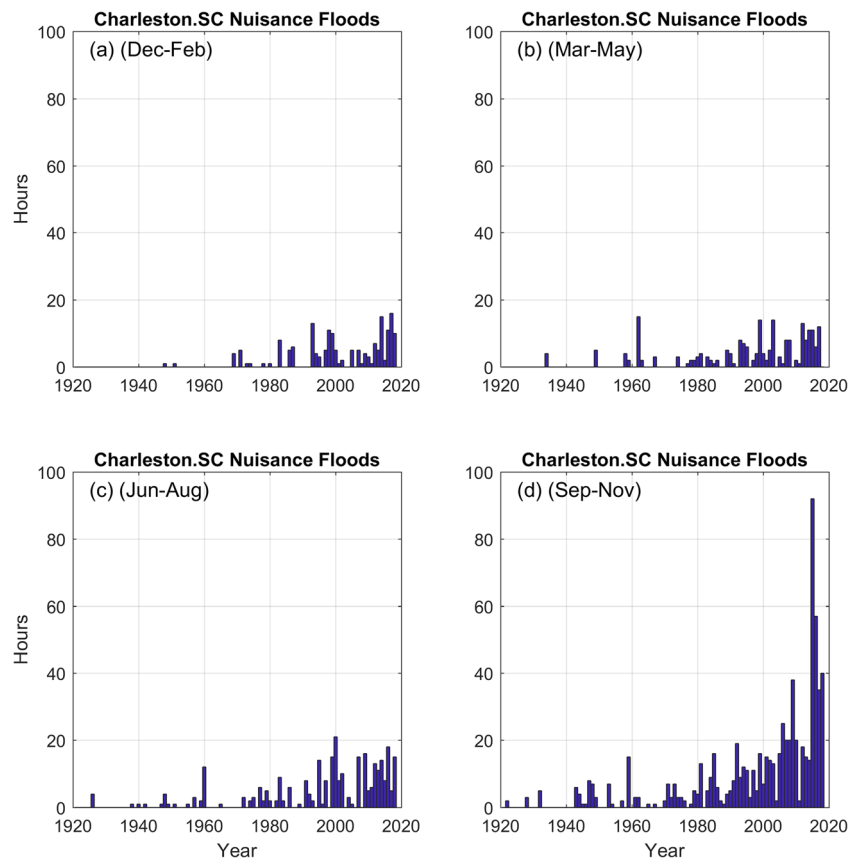
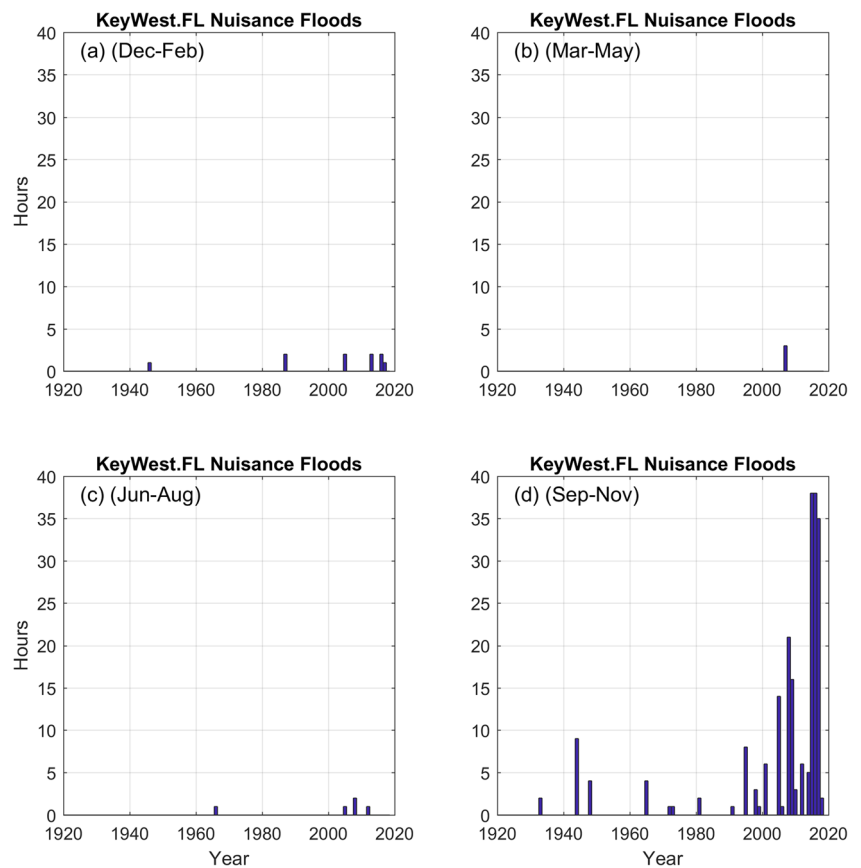


Fig. 8 Same as Fig. 4, but for Key West, FL



when the hourly sea level in Norfolk is ~ 0.1 m higher than the highest spring tide in say February 2018. Due to sea level rise, similar “King Tide” minor flooding in this region has been documented in the fall almost every year in the past decade. For comparison, sea level in Boston (Fig. 11a) is higher in December to January, when an increase in the diurnal spring tide range is seen. Note that the tidal range (MHHW-MLLW) in Boston is 3.13 m and in Norfolk it is only 1.04 m, so tides dominate sea level variability in the GOM more than they are in the MAB.

The tides along the U.S. East Coast are dominated by the lunar semidiurnal M_2 tide (period of 12.42 h), with amplitudes (one half the tidal range) of M_2 as small as 0.186 m in Key west, 0.6–1 m from Florida to New York (but somewhat smaller, 0.366 m in Norfolk) and ~ 1.38 m in Boston and Portland. The relative contribution of the long-term tides is estimated by the ratio between the amplitudes of the annual and semi-annual tides and the semidiurnal tide, $(S_a + S_{sa})/M_2$ (Fig. 12). This relative contribution increases from high to low latitudes, with minimal impact in the GOM where semidiurnal tides are large, to maximum in Key West where semidiurnal tides are very small. In the MAB and SAB regions, the annual and semi-annual tides are ~ 10 –25% of the semidiurnal tide (or ~ 8 –15 cm sea level anomaly). Qualitatively, the contribution of S_a and S_{sa} is

comparable in magnitude to the monthly mean sea level anomaly (Fig. 9) and its timing (Fig. 11) is consistent with the months of maximum mean sea level. To quantify the connection between these long-term tides and mean sea level, the U-TIDE code (Codiga 2011) was used to extract the S_a and S_{sa} constituents from the sea level records of Boston and Norfolk and compare them with the monthly mean sea level at these locations (Fig. 13). The correlation between the monthly mean sea level and the annual and semi-annual tides is very high (~ 0.97), but there are differences between the two locations. The range of the seasonal changes in sea level due to the annual and semi-annual tides is about twice as large in Norfolk (~ 16 cm) as it is in Boston (~ 8 cm); also, the peak of high tide is around May–June in Boston and September–October in Norfolk. In Boston, the long tides match very well with the monthly mean sea level in both, amplitude and phase. However, in Norfolk, the monthly mean range is larger (~ 20 cm) than the tidal contribution and there is some misfit between the tides and mean sea level around June and in September–October. Therefore, it seems that in Norfolk (and other locations in the MAB and SAB, not shown), there are additional contributors to the seasonal pattern; in particular, these additional factors such as tropical storms impact the maximum sea level in September–October.

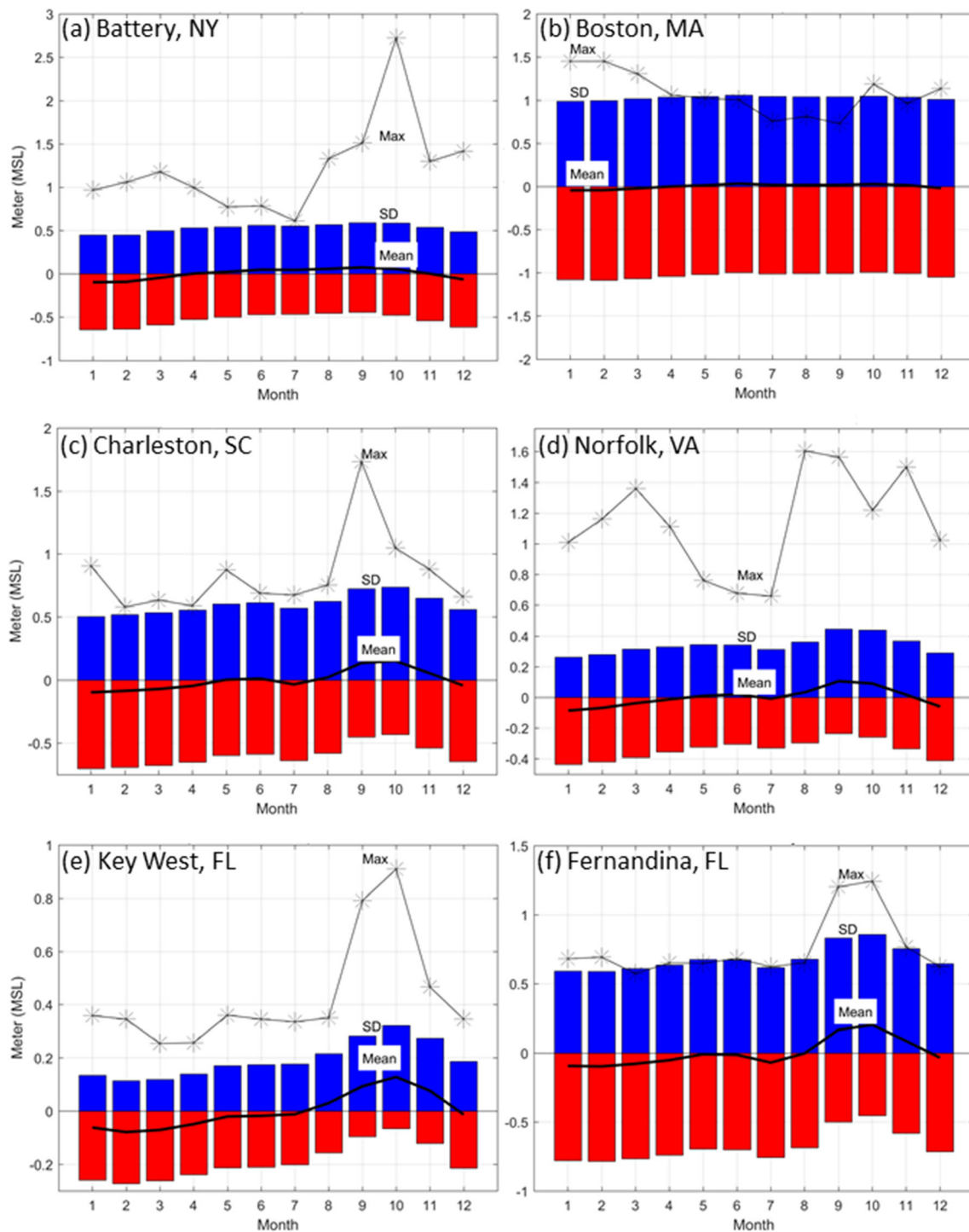


Fig. 9 The monthly mean sea level (heavy black line), standard deviation (blue/red bars for above/below MSL), and maximum values (thin line with stars) for selected stations

3.4 Climatic changes in the wind pattern

Figure 3 indicates that the seasonal pattern of flooding changes over time and these long-term changes are different at different latitudes. A potential contributor for these changes can be a long-term change in the wind pattern. Figure 14 shows the mean zonal wind for 1960–2017 for the same 4 seasons as

defined before; the locations of the 10 tide gauge stations are also shown. Note that the meridional wind component and its changes are much smaller than those of the zonal component, so they are not shown. Eastward blowing winds (westerlies) dominated the northern coastal stations, especially in winter (Fig. 14a), while westward blowing winds (easterlies) dominated the southern stations, more so during fall when the zonal

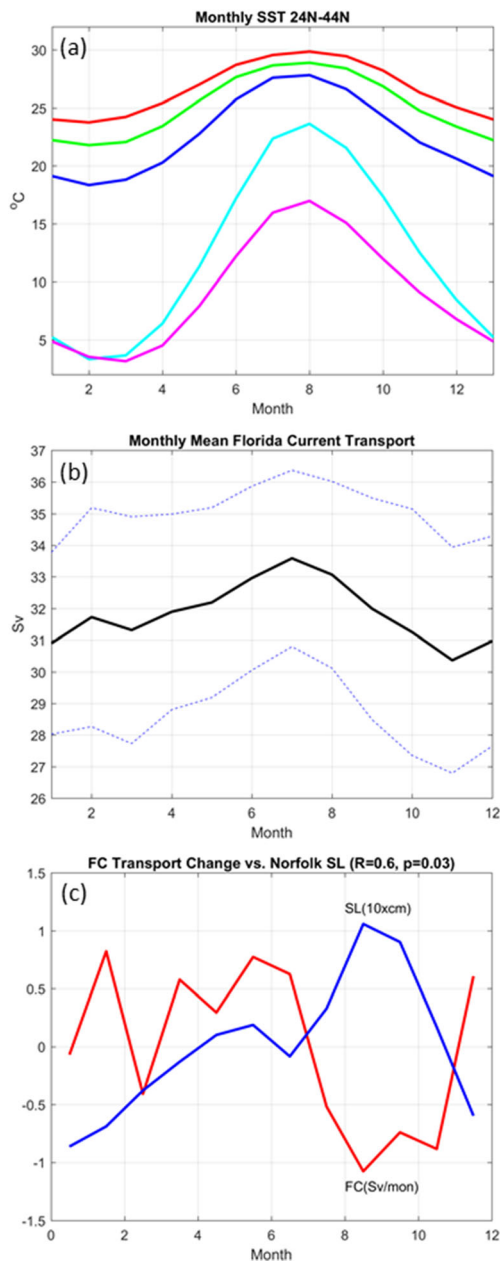


Fig. 10 **a** Monthly mean sea surface temperature (SST) near the U.S. coast at different latitudes (data from NOAA/NCEP reanalysis). **b** Mean and standard deviation (SD) of the monthly Florida Current (FC) transport (cable data from NOAA/AOML). **c** FC transport change from month to month (red; right y-axis) and monthly mean sea level anomaly in Norfolk (blue; left y-axis)

wind shifts northward (Fig. 14d). Therefore, the seasonal wind pattern can further contribute to the higher water levels during the fall, when onshore (easterlies) winds are stronger and the offshore (westerlies) winds move farther north. Figure 15 shows how the seasonal wind pattern changed from 1960–1989 to 1990–2017. The largest change after 1990 is seen during the summer, with an increase in the onshore winds in northern latitudes (~40° N–45° N) and an increase in offshore winds at low latitudes (25° N–30° N) (Fig. 15c). This change

is consistent with the recent increase in summer flooding in Portland and Boston (top two panels of Fig. 3). However, the increase in flooding in the fall south of Battery, New York, cannot be fully explained by changes in wind patterns, which were relatively small during the fall (green color in Fig. 15d at ~27° N–37° N). While changes in wind pattern cannot fully explain the regional changes in flooding, studies of weather patterns over the Northeastern U.S. (Ning and Bradley 2015) show teleconnections with large-scale modes such as NAO and ENSO, so the patterns seen in Fig. 15 are likely part of large-scale patterns. Moreover, Ning and Bradley (2015) also show that the local atmospheric response to the large-scale modes is often different south and north of ~37° N, resembling the latitude that separate regional changes seen here. Connection between long-term changes in NAO and major flooding in Norfolk was also described in Ezer and Atkinson (2014), with an interesting shift between the period 1960–1990 when NAO was generally increasing and 1990–2013 when the NAO was decreasing.

4 Summary and discussion

As sea level continues to rise, the frequency of floods will continue to accelerate along the U.S. coasts (Ezer and Atkinson 2014; Sweet and Park 2014; Sweet et al. 2014; Krueel 2016; Wdowinski et al. 2016). In many places, the so-called nuisance floods already became much more than nuisance, affecting transportation, businesses, real estate values, and in general cause disruption to economic activities of coastal cities and communities (Hino et al. 2019). Addressing challenges in mitigation and adaptation to sea level rise will need regional planning and involvements of the local stakeholders, such as the ongoing efforts in the flood-prone area of the Hampton Roads region of Virginia (Yusuf et al. 2018; John III and Yusuf 2019). However, to address the impact of sea level rise in different regions and predict future changes, better understanding of the spatial and temporal variations of flooding is needed. Here, flooding patterns along the U.S. East Coast are analyzed, focusing on the seasonal variations and how flooding changes from place to place and over time; such information will help in planning regional strategies for adaptation and mitigation. The analysis shows that the seasonal pattern of flooding is changing over time and space in a non-linear and uneven fashion (Fig. 3). Due to the many different drivers that can contribute to seasonal sea level variations and the non-linearity of the system, quantitative linear prediction models may not work well. Because of sea level rise, nuisance flooding becomes more sensitive to various forcing when small changes in mean sea level that in the past were undetected can now able to raise water levels above the flooding threshold during high tides. It is also apparent that minor floods and major floods are not independent of each

Fig. 11 Examples of hourly tide prediction from September, 2017, to March, 2018, for **a** Boston and **b** Norfolk

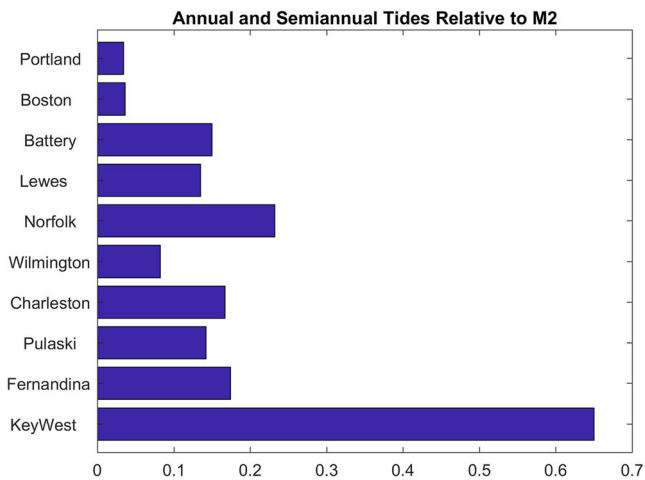
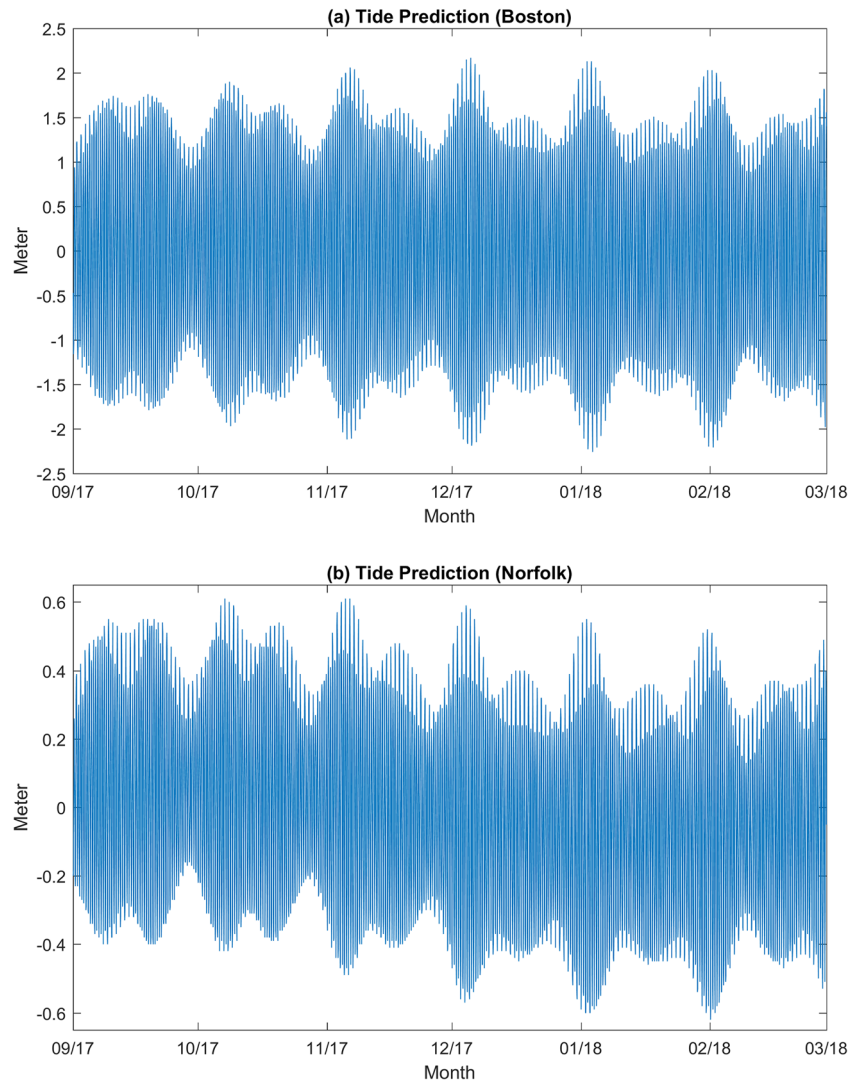


Fig. 12 The ratio between the sum of the amplitudes of the solar annual (S_a) and semi-annual (S_{sa}) tidal constituents and the amplitude of the principal lunar semidiurnal (M_2) constituent

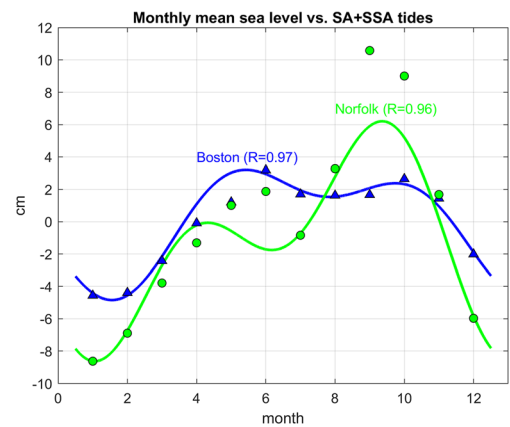
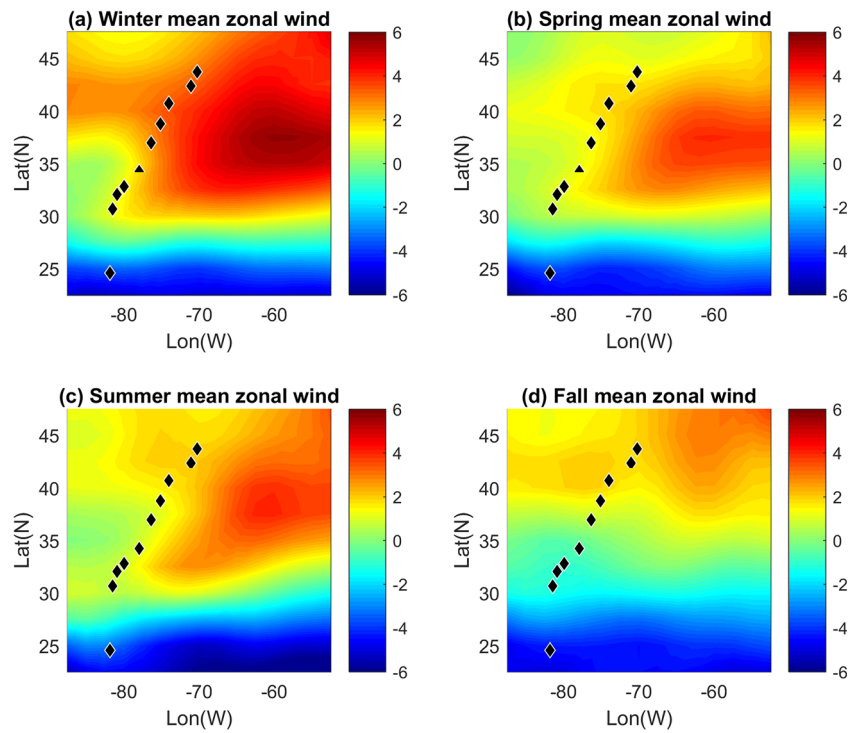


Fig. 13 Monthly mean sea level in Boston (blue triangles) and Norfolk (green circles) versus the combined annual (S_a) and semi-annual (S_{sa}) tides in those locations (solid lines). The monthly means are the same as in Fig. 9 and the tidal constituents are hourly values calculated by U-TIDE

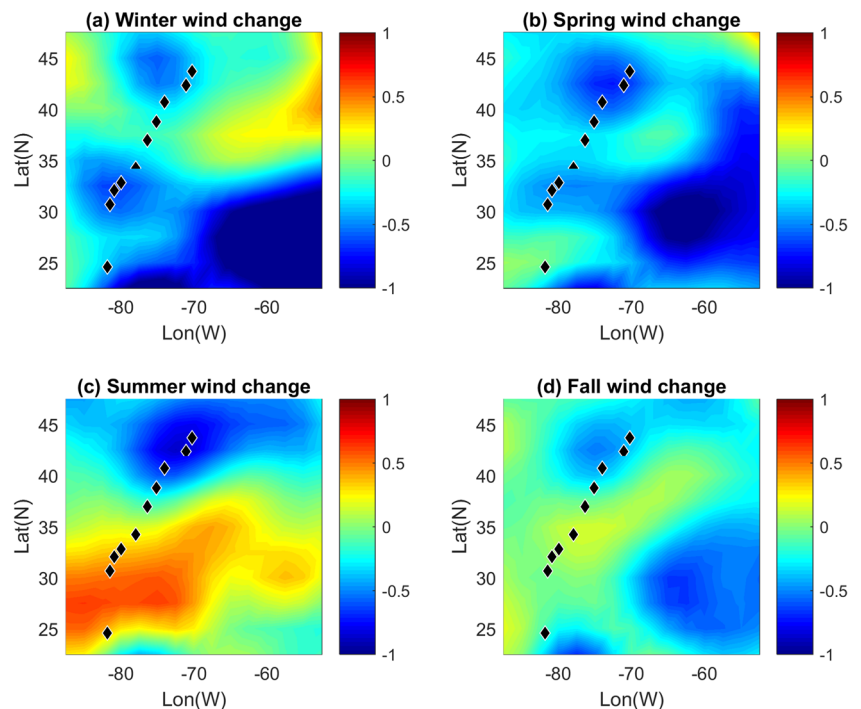
Fig. 14 The mean zonal wind component (m s^{-1}) for the 4 seasons (red/blue for eastward/westward vector direction) from NCEP reanalysis of 1960–2017. Markers show the location of the 10 tide stations of Fig. 1



other. Recent studies show for example that major storm surge floods during hurricanes are often associated with minor tidal flooding in the days after the storm disappeared due to the impact of the storm on ocean dynamics and in particular due to the disruption that the storm can cause to the flow of the Gulf Stream (Ezer et al. 2017; Ezer 2018, 2019a; Todd et al. 2018).

The most noticeable acceleration in flooding was found during the fall for coasts in the MAB and SAB, especially south of New York and all the way down to Key West. There are several potential contributors to this pattern: (1) high water level anomalies in September–October due to the annual and semi-annual tides, (2) weakening of the Gulf Stream during this time, and (3) storm surges due to tropical storms

Fig. 15 Same as Fig. 13, but for the difference between 1990–2017 and 1960–1989 (red/blue indicate increased offshore/onshore wind in recent years)



and hurricanes. The seasonal temperature cycle and associated thermal expansion can also impact mean sea level, but the fact that the maximum SST is in August (when flooding is minimal), while maximum sea level is in September–October, and the fact that the latitudinal change of seasonal SST does not match the spatial variations in sea level, suggest that SST is not the main driver for the seasonal flooding pattern. Note that the different drivers are not independent of each other, so there is no clear cause and effect relation between one dominant forcing and flooding and this study clearly did not cover all the factors involved. For example, the development of tropical storms depends on warm SST, so both can impact sea level, and tropical storms and hurricanes can have both, direct impact on sea level through storm surges, and indirect impact through disruptions to the Gulf Stream flow that then can cause elevated coastal sea level (Ezer et al. 2017; Ezer 2018, 2019a). Higher mean monthly sea level during September–October coincides with increased frequency of storm surges at that time (and increase in extreme sea level; Fig. 9), but it is not clear which factor is the driver and which is the result of the other since mean sea level anomaly and amplitude of storm surges are tightly connected to each other.

On the northeastern coasts, especially in the Gulf of Maine (Boston and Portland), the pattern of seasonal flooding is very different than that found in the SAB and MAB. Since tidal range is large there, seasonal anomaly in mean sea level has relatively small impact. While the amplitude of the annual and semi-annual tides in the GOM are much smaller than the amplitude of the semidiurnal tide, the long-term tides there are nevertheless highly correlated ($R = 0.97$) with the monthly mean sea level which peaks in late spring and early summer. Unlike the large fall flooding in the south, in the GOM, most of the flooding occurred during winter (about half of all the annual flooding) and spring (about a quarter of all the flooding), likely due to winter storms and nor'easters. However, in recent years, the relative contribution of wintertime floods in the north decreases, while summertime and springtime floods increased. The reason could be a shift in zonal wind to a stronger onshore direction during summer after 1990 (Fig. 15c) as well as sea level rise that now started causing summer flooding (which in Boston did not exist at all before ~2008). The long-term shift in wind pattern is likely influenced by large-scale climate modes like NAO and ENSO (Ning and Bradley 2015). It should be acknowledged that several other climate-related changes that could impact the seasonal flooding pattern were not considered here and should be investigated in future studies. These include for example, climatic changes in precipitation and in the hydrological cycle in the Northeastern U.S. (Hayhoe et al. 2007), and long-term changes in the tidal range due to sea level rise (Cheng et al. 2017; Lee et al. 2017). Cheng et al. show, for example, that over the past few decades, M_2 tidal range increased in the GOM and SAB, but decreased in the MAB and the

Chesapeake Bay, and this trend can further impact spatial variations in regional nuisance and tidal flooding.

In summary, the analysis described a complex seasonal pattern that is affected by several different drivers; each of these drivers can change differently over time at different latitudes. Therefore, when planning mitigation and adaptation options one must take a regional approach, taking into account that while the main driver of accelerated flooding is sea level rise, there are other factors that need to be considered such as the long-term tidal cycles, climatic changes in wind patterns and changes in ocean dynamics and circulation.

Acknowledgments The study is part of ODU's Climate Change and Sea Level Rise Initiative and the Institute for Coastal Adaptation and Resilience (ICAR; <https://oduadaptationandresilience.org/>). The Center for Coastal Physical Oceanography (CCPO) provided computational support. The hourly tide gauges sea level data are available from <http://opendap.co-ops.nos.noaa.gov/dods/>. The Florida Current transport data are available from <http://www.aoml.noaa.gov/phod/floridacurrent/>. The SST and wind data are available from <https://www.esrl.noaa.gov/psd/data/gridded/data.ncep.reanalysis.html>.

References

- Baringer MO, Larsen JC (2001) Sixteen years of Florida current transport at 27°N. *Geophys Res Lett* 28(16):3,179–3,182. <https://doi.org/10.1029/2001GL013246>
- Boon JD (2012) Evidence of sea level acceleration at U.S. and Canadian tide stations, Atlantic coast, North America. *J Coast Res* 28(6): 1437–1445. <https://doi.org/10.2112/JCOASTRES-D-12-00102.1>
- Caesar L, Rahmstorf S, Robinson A, Feulner G, Saba V (2018) Observed fingerprint of a weakening Atlantic Ocean overturning circulation. *Nature* 556:191–196. <https://doi.org/10.1038/s41586-018-0006-5>
- Cheng Y, Ezer T, Atkinson LP (2017) Analysis of tidal amplitude changes using the EMD method. *Continental Shelf Res* 148:44–52. <https://doi.org/10.1016/j.csr.2017.09.009>
- Codiga DL (2011) Unified tidal analysis and prediction using the UTide Matlab functions. Technical Report 2011-01. Graduate School of Oceanography, University of Rhode Island, Narragansett, RI. 59pp
- Domingues R, Goni G, Baringer M, Volkov D (2018) What caused the accelerated sea level changes along the U.S. East Coast during 2010–2015? *Geophys Res Lett* 45(24):13,367–13,376. <https://doi.org/10.1029/2018GL081183>
- Ezer T (2013) Sea level rise, spatially uneven and temporally unsteady: why the U.S. East Coast, the global tide gauge record, and the global altimeter data show different trends. *Geophys Res Lett* 40(20): 5439–5444. <https://doi.org/10.1002/2013GL057952>
- Ezer T (2015) Detecting changes in the transport of the Gulf stream and the Atlantic overturning circulation from coastal sea level data: the extreme decline in 2009–2010 and estimated variations for 1935–2012. *Glob Planet Chang* 129:23–36. <https://doi.org/10.1016/j.gloplacha.2015.03.002>
- Ezer T (2016) Can the Gulf Stream induce coherent short-term fluctuations in sea level along the U.S. East Coast? A modeling study. *Ocean Dyn* 66(2):207–220. <https://doi.org/10.1007/s10236-016-0928-0>
- Ezer T (2018) On the interaction between a hurricane, the Gulf Stream and coastal sea level. *Ocean Dyn* 68(10):1259–1272. <https://doi.org/10.1007/s10236-018-1193-1>
- Ezer T (2019a) Numerical modeling of the impact of hurricanes on ocean dynamics: sensitivity of the Gulf Stream response to storm's track.

- Ocean Dyn 69(9):1053–1066. <https://doi.org/10.1007/s10236-019-01289-9>
- Ezer T (2019b) Regional differences in sea level rise between the Mid-Atlantic Bight and the South Atlantic Bight: is the Gulf Stream to blame? *Earth's Future* 7(7):771–783. <https://doi.org/10.1029/2019EF001174>
- Ezer T, Atkinson LP (2014) Accelerated flooding along the U.S. East Coast: on the impact of sea-level rise, tides, storms, the Gulf stream, and the North Atlantic Oscillations. *Earth's Future* 2(8):362–382. <https://doi.org/10.1002/2014EF000252>
- Ezer T, Atkinson LP (2017) On the predictability of high water level along the U.S. East Coast: can the Florida Current measurement be an indicator for flooding caused by remote forcing? *Ocean Dyn* 67(6):751–766. <https://doi.org/10.1007/s10236-017-1057-0>
- Ezer T, Corlett WB (2012) Is sea level rise accelerating in the Chesapeake Bay? A demonstration of a novel new approach for analyzing sea level data. *Geophys Res Lett* 39(19). <https://doi.org/10.1029/2012GL053435>
- Ezer T, Atkinson LP, Corlett WB, Blanco JL (2013) Gulf stream's induced sea level rise and variability along the U.S. mid-Atlantic coast. *J Geophys Res* 118:685–697. <https://doi.org/10.1002/jgrc.20091>
- Ezer T, Atkinson LP, Tuleya R (2017) Observations and operational model simulations reveal the impact of Hurricane Matthew (2016) on the Gulf Stream and coastal sea level. *Dyn Atmos Oceans* 80: 124–138. <https://doi.org/10.1016/j.dynatmoce.2017.10.006>
- Goddard PB, Yin J, Griffies SM, Zhang S (2015) An extreme event of sea-level rise along the northeast coast of North America in 2009–2010. *Nat Commun* 6:6345. <https://doi.org/10.1038/ncomms7346>
- Hall T, Booth JF (2017) SynhETC: a statistical model for severe winter storm hazard on Eastern North America. *J Clim* 30:5329–5343. <https://doi.org/10.1175/JCLI-D-16-0711.1>
- Hayhoe K, Wake CP, Huntington TG, Luo L, Schwartz MD, Sheffield J, Wood E, Anderson B, Bradbury J, DeGaetano A, Troy TJ, Wolfe D (2007) Past and future changes in climate and hydrological indicators in the US Northeast. *Clim Dyn* 28(4):381–407. <https://doi.org/10.1007/s00382-006-0187-8>
- Hino M, Belanger ST, Field CB, Davies AR, Mach KJ (2019) High-tide flooding disrupts local economic activity. *Science Adv* 5(2). <https://doi.org/10.1126/sciadv.aau2736>
- John SB III, Yusuf JE (2019) Perspectives of the expert and experienced on challenges to regional adaptation for sea level rise: implications for multisectoral readiness and boundary spanning. *Coast Manag* 47(2):151–168. <https://doi.org/10.1080/08920753.2019.1564951>
- Kruel S (2016) The impacts of sea-level rise on tidal flooding in Boston, Massachusetts. *J Coast Res* 32(6):1302–1309. <https://doi.org/10.2112/JCOASTRES-D-15-00100.1>
- Lee SB, Li M, Zhang F (2017) Impact of sea level rise on tidal range in Chesapeake and Delaware bays. *J Geophys Res* 122(5):3917–3938. <https://doi.org/10.1002/2016JC012597>
- Loftis JD, Forrest D, Katragadda S, Spencer K, Organski T, Nguyen C, Rhee S (2018) StormSense: a new integrated network of IoT water level sensors in the smart cities of Hampton Roads, VA. *Mar Technol Soc J* 52(2):56–67. <https://doi.org/10.4031/MTSJ.52.2.7>
- Meinen CS, Baringer MO, Garcia RF (2010) Florida current transport variability: an analysis of annual and longer-period signals. *Deep Sea Res* 57(7):835–846. <https://doi.org/10.1016/j.dsr.2010.04.001>
- Ning L, Bradley RS (2015) Winter climate extremes over the northeastern United States and southeastern Canada and teleconnections with large-scale modes of climate variability. *J Clim* 28:2475–2493. <https://doi.org/10.1175/JCLI-D-13-00750.1>
- Park J, Sweet W (2015) Accelerated sea level rise and Florida current transport. *Ocean Sci* 11:607–615. <https://doi.org/10.5194/os-11-607-2015>
- Pawlowicz R, Beardsley B, Lentz S (2002) Classical tidal harmonic analysis including error estimates in MATLAB using T-TIDE. *Comput Geosci* 28(8):929–937. [https://doi.org/10.1016/S0098-3004\(02\)00013-4](https://doi.org/10.1016/S0098-3004(02)00013-4)
- Piecuch CG, Dangendorf S, Ponte R, Marcos M (2016) Annual sea level changes on the North American Northeast Coast: influence of local winds and barotropic motions. *J Clim* 29:4801–4816. <https://doi.org/10.1175/JCLI-D-16-0048.1>
- Piecuch CG, Dangendorf S, Gawarkiewicz GG, Little CM, Ponte RM, Yang J (2019) How is New England coastal sea level related to the Atlantic meridional overturning circulation at 26°N? *Geophys Res Lett* 46(10):5351–5360. <https://doi.org/10.1029/2019GL083073>
- Sallenger AH, Doran KS, Howd P (2012) Hotspot of accelerated sea-level rise on the Atlantic coast of North America. *Nat Clim Chang* 2:884–888. <https://doi.org/10.1038/NCILMATE1597>
- Sweet W, Park J (2014) From the extreme to the mean: acceleration and tipping points of coastal inundation from sea level rise. *Earth's Future* 2(12):579–600. <https://doi.org/10.1002/2014EF000272>
- Sweet W, Park J, Marra J, Zervas C, Gill S (2014) Sea level rise and nuisance flood frequency changes around the United States. NOAA Technical report NOS CO-OPS 073, NOAA Silver Spring, MD, 58 pp.
- Sweet W, Dusek G, Obeysekera J, Marra JJ (2018) Patterns and projections of high tide flooding along the U.S. coastline using a common impact threshold. NOAA Technical report NOS CO-OPS 086, NOAA Silver Spring, MD, 44 pp.
- Todd RE, Asher TG, Heiderich J, Bane JM, Luettich RA (2018) Transient response of the Gulf Stream to multiple hurricanes in 2017. *Geophys Res Lett* 45. <https://doi.org/10.1029/2018GL079180>
- Valle-Levinson A, Dutton A, Martin JB (2017) Spatial and temporal variability of sea level rise hot spots over the eastern United States. *Geophys Res Lett* 44:7876–7882. <https://doi.org/10.1002/2017GL073926>
- Wdowinski S, Bray R, Kirtman BP, Wu Z (2016) Increasing flooding hazard in coastal communities due to rising sea level: case study of Miami Beach, Florida. *Ocean Coast Manag* 126:1–8. <https://doi.org/10.1016/j.ocecoaman.2016.03.002>
- Woodworth PL, Maqueda MM, Gehrels WR, Roussenov VM, Williams RG, Hughes CW (2016) Variations in the difference between mean sea level measured either side of Cape Hatteras and their relation to the North Atlantic Oscillation. *Clim Dyn* 49(7–8):2451–2469. <https://doi.org/10.1007/s00382-016-3464-1>
- Yusuf JE, John BS III, Covi M, Nicula JG (2018) Engaging stakeholders in planning for sea level rise and resilience. *J Contemp Water Res Educ* 164(1):112–123. <https://doi.org/10.1111/j.1936-704X.2018.03287.x>